



Electrochemical and Spectroelectrochemical Characterization of Bacteria and Bacterial Systems

Journal:	<i>Analyst</i>
Manuscript ID	AN-MRV-10-2021-001954.R1
Article Type:	Minireview
Date Submitted by the Author:	23-Nov-2021
Complete List of Authors:	Sundaresan, Vignesh; University of Notre Dame, Chemical and Biomolecular Engineering Do, Hyein; University of Notre Dame, Department of Chemistry and Biochemistry Shrout, Joshua; University of Notre Dame, Department of Civil and Environmental Engineering and Earth Sciences Bohn, Paul; University of Notre Dame, Department of Chemical and Biomolecular Engineering

1
2
3 **Electrochemical and Spectroelectrochemical Characterization of Bacteria and Bacterial**
4
5 **Systems**
6

7 Vignesh Sundaresan¹, Hyein Do², Joshua D. Shroust^{3,4,5}, and Paul W. Bohn^{1,2*}
8
9

10
11
12 ¹Department of Chemical and Biomolecular Engineering, University of Notre Dame, Notre
13
14 Dame, IN 46556 USA
15

16
17 ²Department of Chemistry and Biochemistry, University of Notre Dame, Notre Dame, IN 46556
18
19 USA
20

21
22 ³Department of Civil and Environmental Engineering and Earth Sciences, University of Notre
23
24 Dame, Notre Dame, IN 46556 USA
25

26
27 ⁴Eck Institute for Global Health, University of Notre Dame, Notre Dame, IN 46556 USA
28

29
30 ⁵Department of Biological Sciences, University of Notre Dame, Notre Dame, IN 46556 USA
31
32
33
34
35
36
37
38
39
40
41
42
43
44
45
46
47
48
49
50
51
52
53
54
55
56
57
58

Abstract

Microbes, such as bacteria, can be described, at one level, as small, self-sustaining chemical factories. Based on the species, strain, and even the environment, bacteria can be useful, neutral or pathogenic to human life, so it is increasingly important that we be able to characterize them at the molecular level with chemical specificity and spatial and temporal resolution in order to understand their behavior. Bacterial metabolism involves a large number of internal and external electron transfer processes, so it is logical that electrochemical techniques have been employed to investigate these bacterial metabolites. In this mini-review, we focus on electrochemical and spectroelectrochemical methods that have been developed and used specifically to chemically characterize bacteria and their behavior. First, we discuss the latest mechanistic insights and current understanding of microbial electron transfer, including both direct and mediated electron transfer. Second, we summarize progress on approaches to spatiotemporal characterization of secreted factors, including both metabolites and signaling molecules, which can be used to discern how natural or external factors can alter metabolic states of bacterial cells and change either their individual or collective behavior. Finally, we address *in situ* methods of single-cell characterization, which can uncover how heterogeneity in cell behavior is reflected in the behavior and properties of collections of bacteria, *e.g.* bacterial communities. Recent advances in (spectro)electrochemical characterization of bacteria have yielded important new insights both at the ensemble and the single-entity levels, which are furthering our understanding of bacterial behavior. These insights, in turn, promise to benefit applications ranging from biosensors to the use of bacteria in bacteria-based bioenergy generation and storage.

Introduction

Microorganisms are tremendously important to human life, both because of our symbiotic relationships with them and for their utility in many areas of technology, such as food sciences, biomedicine and genetic engineering.¹ On the other hand, microbial exposure can lead to deleterious outcomes ranging from the unpleasant, *e.g.* body odor, to the life threatening, *e.g.* systemic inflammatory response syndrome.² As just one example, a broad range of microbes, including bacteria, molds, and yeasts, are used in food production, yet some bacteria contribute to contamination and food spoilage.^{3, 4} In the context of human health, there are *ca.* 1,400 known species of human pathogens, spanning bacteria, viruses, and fungi, and some of the bacterial pathogens responsible for high mortality and morbidity, *e.g.* *Streptococcus pneumoniae* and *Pseudomonas aeruginosa*.⁵⁻⁷ Therefore, the problem of microbial characterization has two main components: (1) the ability to detect and identify microbes at the species, and even strain, level in order to correlate them with pathogenic exposure, and (2) developing tools to better understand the molecular underpinnings of microbial behavior, including the structures, metabolites, electron transfer mechanisms, that collectively determine their functional characteristics.^{1, 8} The detection and identification of microbial species, especially pathogens, is an area of intense investigation that has been the subject of a number of recent reviews.⁹⁻¹¹ Therefore, this mini-review will concentrate on the second area - specifically on electrochemical and spectroelectrochemical means of elucidating microbial behavior at the molecular level.

A wide range of analytical methods have been applied for detecting and analyzing microbes, depending on the purpose and the level of information needed.¹² Some techniques have been developed for rapid and reliable bacterial identification, *e.g.* polymerase chain reaction-based methods,¹³⁻¹⁵ mass spectrometry,¹⁶⁻¹⁸ flow cytometry,^{19, 20} and fluorescence immunoassay.²¹⁻²³ In

1
2
3 the last two decades, absorption, scattering, and vibrational techniques, *e.g.* uv-visible absorption,
4 Raman, and Fourier-transform infrared (FTIR) spectroscopies, have demonstrated their great
5 utility in microbial identification and have also been applied to obtain detailed information on the
6 chemical composition of complex heterogeneous microbial systems.²⁴⁻²⁶ In addition to being non-
7 destructive, label-free, and needing only minimal sample pretreatment, both IR and Raman spectra
8 provide spectral fingerprints, thus delivering comprehensive chemical information about the main
9 characteristics of biological systems at the molecular level.^{26, 27} As just two examples, our group
10 has used confocal Raman hyperspectral imaging to characterize how *P. aeruginosa* signaling
11 molecules respond to different environmental conditions in both two- and three-dimensions,^{28, 29}
12 and Holman and coworkers used FTIR spectromicroscopy to monitor and characterize *Escherichia*
13 *coli* biofilm activity at a molecular level over long times.³⁰

14
15
16
17
18
19
20
21
22
23
24
25
26
27
28
29
30
31
32
33
34
35
36
37
38
39
40
41
42
43
44
45
46
47
48
49
50
51
52
53
54
55
56
57
58
59
60

Electrochemical methods, which have also been widely used to investigate microbial systems, are particularly powerful, because they provide information that is complementary to spectroscopy, especially those involving the redox properties of microbial analytes. Electrochemical approaches, in general, provide rapid response times, simple operation, good sensitivity, and are cost-efficient.^{31, 32} Generally, bacteria can transport electrons across their cell membrane such that they electrically interact with their environment.³³ Therefore, electrochemical methods have the advantage of being able to explore the interaction between an electrode surface and living microbial cells, which is especially useful, for example, in applications such as electricity production and bioremediation.^{34, 35} In addition, electrochemical approaches can address both technological useful applications, such as microbial fuel cells, as well as potentially harmful processes such as bacterial-initiated metal corrosion.³⁵⁻³⁷ Recently, Simoska *et al.* demonstrated *in vitro* detection of three redox-active phenazine metabolites from the opportunistic human pathogen

1
2
3 *P. aeruginosa* using carbon-based ultramicroelectrode (UME) sensing electrodes to monitor and
4 characterize the production of the phenazines in real-time.³⁸ Qiao *et al.* demonstrated that *E. coli*
5 evolves under electrochemical tension in a microbial fuel cell in a such a way that it secretes
6 hydroquinone derivatives through a highly permeable outer membrane, which then act as
7 mediators for electron transport between cell and electrode.³⁹
8
9

10
11
12
13
14
15
16
17
18
19
20
21
22
23
24
25
26
27
28
29
30
31
32
33
34
35
36
37
38
39
40
41
42
43
44
45
46
47
48
49
50
51
52
53
54
55
56
57
58
59
60

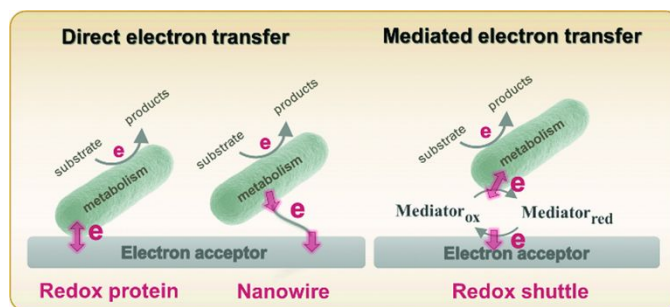
These examples, and those to be discussed below, illustrate the ability of electrochemical techniques to rapidly provide quantitative information about electroactive species. However, electrochemistry is limited in providing information about molecular structure. This provides powerful motivation for coupling electrochemistry with spectroscopy, since the two approaches generally offer complementary information. For example, changes in spectral line profiles, reflecting changes in the electronic structure of the molecule, are typically observed when the redox state is changed electrochemically.^{40, 41} This feature has driven the application of spectroelectrochemical approaches in microbial sciences - targeting species as diverse as redox enzymes, electroactive bacteria, and microbial biofilms.^{40, 42-44}

In this review, we describe how electrochemical and spectroelectrochemical approaches are useful in understanding the characteristics of bacteria at both ensemble and single-entity levels. The review is meant to highlight the way in which advanced spectroelectrochemical measurements can be used to discern important operational characteristics of complex microbial electron transfer systems. It is specifically not intended to be an exhaustive or comprehensive examination of microbial external electron transfer (EET) for which other excellent recent reviews are available.⁴⁵⁻⁴⁸ The review is organized in three sections. In the first, we discuss recent mechanistic insights obtained on direct and mediated electron transfer processes occurring in bacteria. The discussion on direct electron transfer is exemplified by electron transport in *Geobacter sulfurreducens*

whereas, the discussion of mediated electron transfer focuses on the necessary attributes of redox mediators. Next, we discuss how (spectro)electrochemical methods can be used to analyze the spatiotemporal distribution of secreted metabolites in order to understand the manner in which bacteria sense and react to their environment, by using *P. aeruginosa* as an example. In the final section, we describe how (spectro)electrochemical strategies have been exploited to study single bacterial cells. While earlier reports are highlighted to provide historical context, the primary emphasis is on papers published in the past five years.

Microbial electron transfer

Metabolism in bacteria can be regulated by internal or external electron transfer events, or by a combination of the two. A great deal of attention has been given to external electron transfer (EET) because it's direct relevance in fields such as microbial fuel cells, corrosion, and sensors.⁴⁹⁻
⁵¹ EET can occur in microbes by one of two mechanisms: (1) direct electron transfer (**Figure 1, left**), in which electron transfer occurs through membrane-associated redox proteins, and (2) mediated electron transfer (**Figure 1, right**), in which electron transfer between the cell membrane and electrode occurs through the agency of a redox mediator.⁵² Since there are recent reviews focusing on EET as it relates to microbial fuel cells,^{49, 50, 53} corrosion^{51, 54, 55} and sensors,^{32, 56} here we discuss only the recent advances in developing mechanistic understanding of EET using electrochemical and spectroelectrochemical methods.



1
2
3 **Figure 1.** Schematic diagram describing direct (*left*) and mediated (*right*) electron transfer in the
4 microbial system. Adapted with permission from reference ⁵⁷. Copyright 2020 Progress in
5 Chemistry.
6
7
8
9

10 *Direct electron transfer.* Direct electron transfer between the bacterial cell and electrode
11 typically occurs via one of three mechanisms: through (1) redox proteins, such as C-type
12 cytochromes and flavoproteins, (2) conductive pili, and (3) endogenously produced mediators that
13 are bound to the cell membrane.⁴⁹ Mechanistic understanding of the direct electron transfer process
14 is important in order to improve understanding of bacterial metabolism and better design
15 bioelectrochemical systems, and also as a starting point for the development of engineered redox
16 proteins bound to the cell membrane.
17
18
19
20
21
22
23
24
25
26

27 Owing to its ability to form thick biofilms and conduct long-distance electron transport,
28 *Geobacter sulfurreducens* is commonly used in bioelectrochemical systems, specifically microbial
29 fuel cells.^{58, 59} EET occurs in *G. sulfurreducens* through membrane-resident c-type cytochromes
30 and/or conductive pili.⁶⁰⁻⁶³ Electrochemical methods have been used to decipher the EET
31 mechanism, track biofilm formation, and identify the charge state of the cells. For example, open
32 circuit potentiometry was used to measure the charge stored in *G. sulfurreducens*.⁶⁴ The results
33 indicated three cytochrome proteins in the periplasm capable of storing charges. Rova and co-
34 workers developed a dynamic model for EET in *G. sulfurreducens* using data obtained by a
35 combination of *in situ* resonance Raman microscopy and chronoamperometry. Using this
36 approach, they were able to calculate quantitative rate constants for electron transfer at different
37 steps from the inner membrane to the electrode surface.⁶⁵ Interestingly, *G. sulfurreducens* can be
38 used for both anodic and cathodic bioelectrochemical systems. While the electron transfer
39 mechanism of the anodic reaction, which occurs via cytochromes in the membrane and/or pili is
40
41
42
43
44
45
46
47
48
49
50
51
52
53
54
55
56
57
58
59
60

1
2
3 reasonably well-understood, a deeper mechanistic understanding of the cathodic electron transfer
4
5 process is needed.
6
7

8
9 Reisner and co-workers addressed this issue spectroelectrochemically by employing *in situ*
10
11 resonance Raman spectroscopy and uv-visible absorption in both anodic and cathodic
12
13 environments.⁶⁶ First, anodically-grown *G. sulfurreducens* biofilms were interrogated for their
14
15 activity towards oxidation of acetate to CO₂. Then, the same biofilm containing electrode was
16
17 operated in cathodic mode for the reduction of fumarate to succinate. The corresponding cyclic
18
19 voltammograms of both anodic (**Figure 2A**) and cathodic (**Figure 2B**) modes show expected
20
21 sigmoidal responses indicating reversible redox reactions. The uv-visible absorption spectrum
22
23 (**Figure 2C**) exhibits Soret bands at 409 and 419 nm in anodic mode, which are associated with
24
25 the heme-type cytochromes. However, these bands disappear in cathodic mode, indicating the
26
27 depletion of cytochromes at more negative potentials. Moreover, the electrode becomes red and
28
29 increasingly darker over multiple cathodic cycles, and resonance Raman spectroscopy and electron
30
31 microscopy suggest the presence of iron oxide nanoparticles on or near the cells. Taken together,
32
33 the authors proposed that the EET in anodic mode occurs mainly via cytochromes, while EET in
34
35 cathodic mode could be mediated by iron species and/or iron oxide nanoparticles produced by
36
37 heme-containing cytochromes, as shown in **Figure 2D**. Similarly, Yi *et al.* used electrochemical
38
39 methods to study the mechanism of EET in *Shewanella loihica*, which is also capable of
40
41 bidirectional electron transport.⁶⁷ They postulated that riboflavin acts as a redox mediator in two
42
43 different modes - freely diffusing for outward EET (electron transfer from bacteria to the
44
45 electrode), or as a bound species for inward EET (electron transfer from the electrode to bacteria).
46
47 Spectroelectrochemical studies have also been used to understand direct interspecies electron
48
49 transfer (electron transfer directly between bacterial species) in *Geobacter* co-cultures involving
50
51
52
53
54
55
56
57
58

Geobacter metallireducens and *G. sulfurreducens*.⁶⁸ *In situ* Raman scattering and FTIR revealed that interspecies electron transport is mediated by c-type cytochromes. Additionally, electrochemical studies and confocal laser scanning microscopy imaging with a pilR-deficient *G. sulfurreducens* mutant showed that this mutant strain forms thinner and less conductive biofilms, giving support to the importance of PilR in regulating PilA and overall type IV pilus (TFP) appendage production, as TFP are known to have important roles in biofilm formation and EETs.⁶⁹

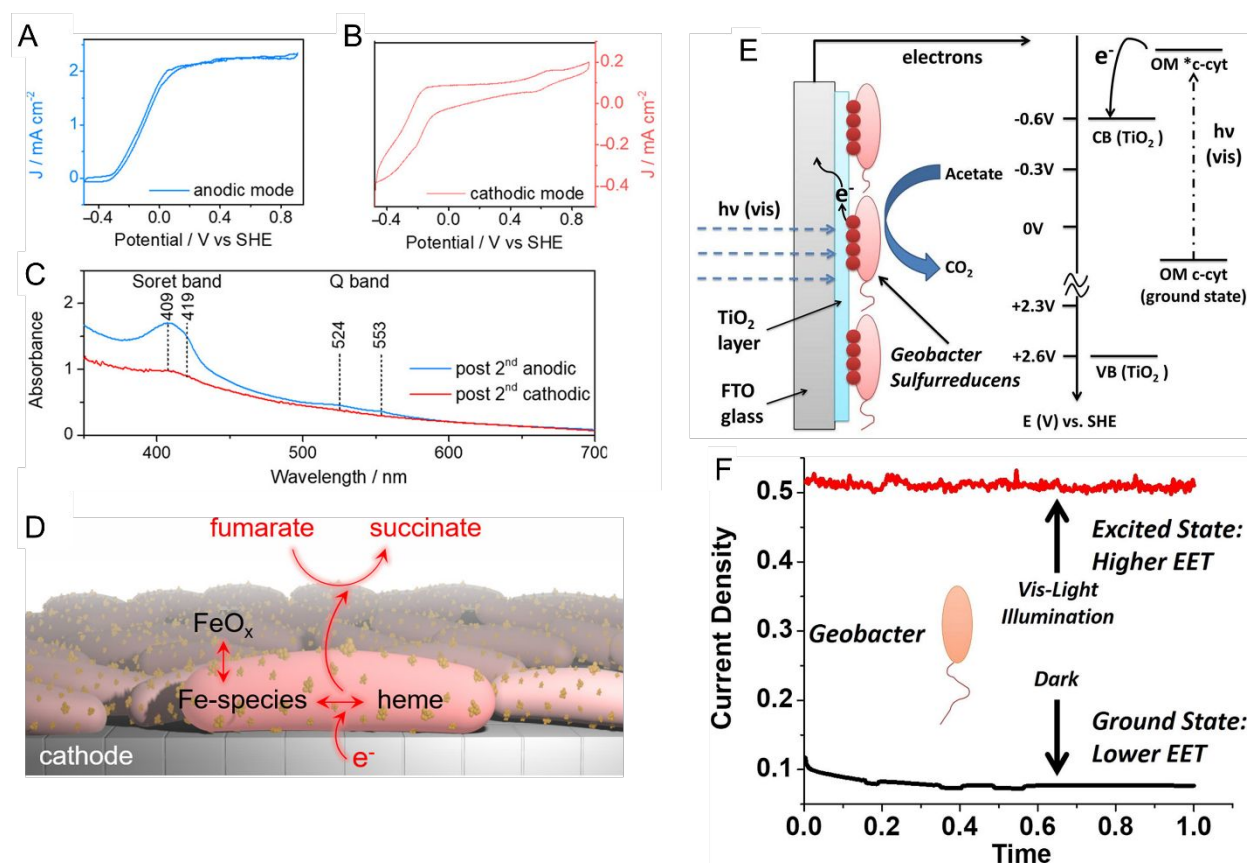


Figure 2. Cyclic voltammograms of a *G. sulfurreducens* biofilm on an indium-tin-oxide (ITO) electrode in (A) anodic (acetate to CO_2) and (B) cathodic (fumarate to succinate) modes. (C) UV-visible spectra of biofilms after anodic and cathodic scans. (D) Schematic illustrating plausible EET mechanism in cathodic mode. (E) Schematic and energy diagram showing EET from *G. sulfurreducens* directly to TiO_2 under visible illumination. OM = outer membrane. (F) Current density obtained from *G. sulfurreducens* under dark and illuminated conditions. Panels A-D are adapted with permission from ref⁶⁶. Copyright 2020 American Chemical Society. Panel E and F are adapted with permission from ref⁷⁰. Copyright 2020 Elsevier B.V.

1
2
3 Recent reports suggest that visible light can play an important role in dictating the electron
4 transfer through cell membrane proteins. For example, Zhang *et al.* show that visible illumination
5 of *G. sulfurreducens* can excite c-type cytochromes (OM c-cyts) in the cell membrane to an energy
6 level high enough to easily transfer electrons to TiO₂ as shown in **Figure 2E**.⁷⁰ This visible-light
7 driven approach produced an 8× improvement in EET as compared to the non-illuminated
8 condition (**Figure 2F**). Apart from enhancing the EET using light, Tefft and TerAvest showed that
9 illuminating *Shewanella oneidensis* with green light can generate a proton pump or proton motive
10 force within the cell, which can reverse the direction of electron transfer such that electrons can be
11 transferred from the cathode to a proximal bacterial cell for reduction.⁷¹ These reports highlight
12 how visible light can be used to improve and manipulate EET, enabling the design of
13 bioelectrochemical systems with enhanced performance. Apart from *G. sulfurreducens*,
14 electrochemical and spectroelectrochemical methods have been used to understand and
15 characterize a wide variety of bacteria under a wide variety of other conditions,⁷²⁻⁷⁸ including
16 recognizing EETs in mammalian gut microbiota,⁷³ and long-distance electron transfer in a Gram-
17 positive bacterium, *Lysinibacillus* isolate GY32.⁷²

18
19
20
21
22
23
24
25
26
27
28
29
30
31
32
33
34
35
36
37
38
39
40
41
42
43
44
45
46
47
48
49
50
51
52
53
54
55
56
57
58
59
60
Mediated electron transfer. Most bacteria do not contain accessible redox-active species
in their (outer) membrane and even in bacteria that do, transferring electrons directly via
membrane-resident redox proteins is challenging because of factors like poorly electrically
conducting cell membranes, and inaccessibility to redox proteins.^{79, 80} To overcome these issues,
redox mediators have been employed to shuttle electrons from the electrode to the bacterial redox
site and *vice versa*.⁸¹⁻⁸³ Redox mediators play an important role not only in accelerating EET
processes but also in enhancing the efficiency of bioelectrochemical systems. Some of the
commonly encountered redox mediators utilized by different bacteria include flavins, quinones,

1
2
3 and phenazines.^{81, 84, 85} Both voltammetric and amperometric methods have been used to examine
4
5 the redox mediator competency and its interaction with the bacterial cell.⁸⁶⁻⁸⁸ Recently, Minter
6
7 and co-workers performed a comprehensive electrochemical study to understand the phenazine-
8
9 based redox mediators and their interaction with *E. coli*.⁸⁸ They employed nine different
10
11 phenazine-based redox mediators, out of which neutral red (NR) exhibited the highest current
12
13 density, as shown in **Figure 3A**. Additionally, cytotoxicity studies showed that NR did not affect
14
15 cell growth in this system. Expanding to all mediators, the measured current densities can be
16
17 correlated to cytotoxicity to an extent that dictates that redox potential is not the only criteria in
18
19 choosing redox mediators. Analogously, Liu and co-workers studied the effect of redox mediators
20
21 on *S. oneidensis* MR-1 biofilm formation.⁸⁹ Even though previous reports showed that redox
22
23 mediators promote biofilm formation, the mechanisms by which this occurs are poorly understood.
24
25 The authors employed five different redox mediators, all of which promoted biofilm formation as
26
27 evident by both the increase in current density (**Figure 3B**) and the robust morphology shown in
28
29 the SEM images (**Figure 3C**). The improvement in EET efficiency was attributed to synergies
30
31 between mediators promoting biofilm formation and upregulating gene expression for cell
32
33 membrane constituents. In some cases, endogenously produced molecules can mediate electron
34
35 transfer.⁹⁰⁻⁹² For example, Mulla and co-workers showed that at elevated temperatures (55 °C),
36
37 thermophilic *Geobacillus* sp. produce extracellular polysaccharide (EPS) which contains flavins
38
39 that mediate EET.⁹³ In addition, Zhuang and co-workers showed that the production and
40
41 composition of EPS can be controlled by the application of oxidizing potentials in a mixed
42
43 community biofilm.⁹⁴
44
45
46
47
48
49
50

51
52 Augmenting traditional redox mediators, Liu *et al.* demonstrated that bacterial vesicles can
53
54 also mediate EET.⁹⁵ Several Gram-negative bacteria release outer membrane vesicles (OMVs) that
55
56
57
58

1
2
3 contain c-type cytochromes which facilitate electron transfer. Electrochemical studies showed a ~
4
5 1.7x enhancement in current density when OMVs were used as mediators (**Figure 3D**).
6
7 Additionally, OMVs can enable electron transport in non-exoelectrogens including *E. coli*. It is
8
9 important to note that a variety of bacteria secrete redox-active metabolites, which can also be used
10
11 as mediators. Clearly, characterizing these metabolites would do much to enable the understanding
12
13 of metabolic state, as discussed in the next section.
14
15
16
17

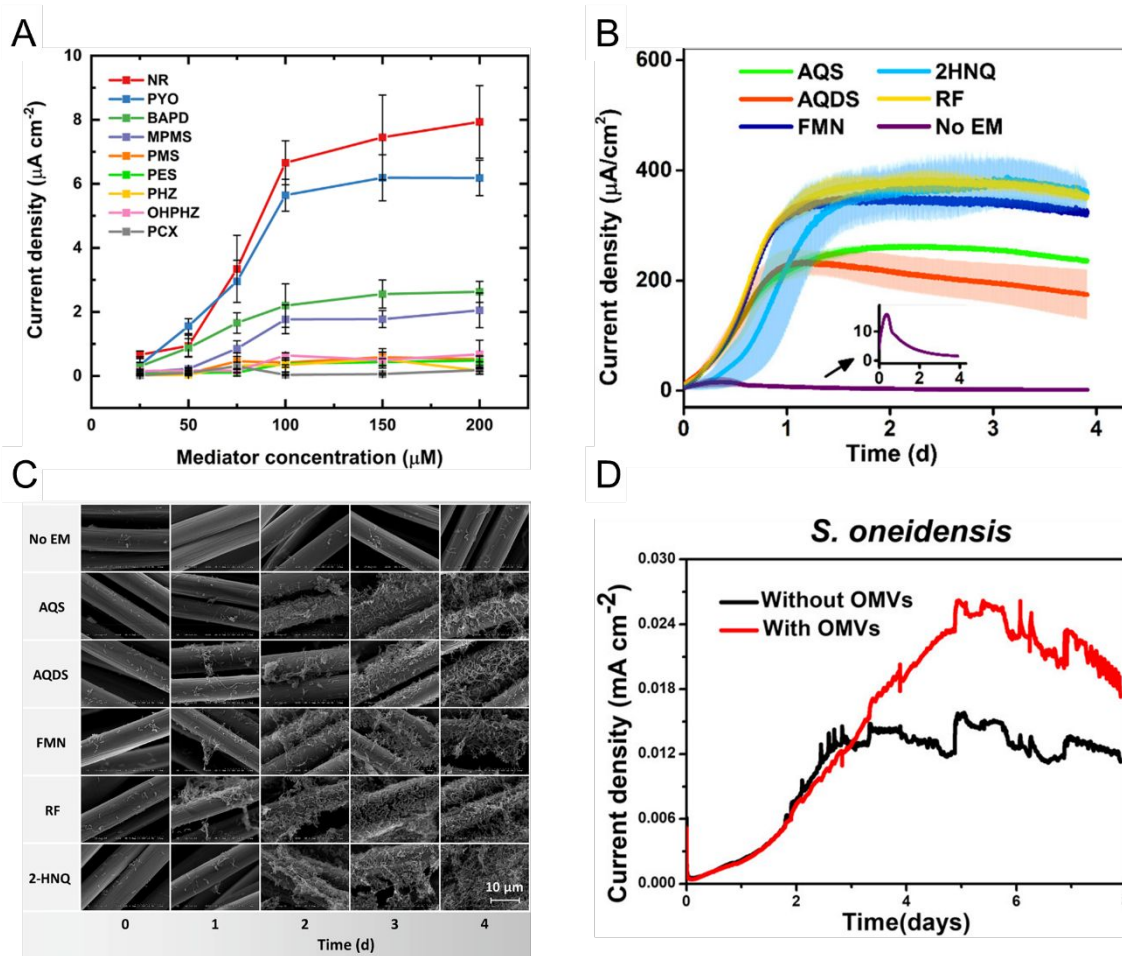


Figure 3. (A) Current densities obtained from *E. coli* immobilized on carbon paper electrode with nine different redox mediators at six different concentrations. NR: neutral red, PYO: pyocyanin, BAPD: benzo(A)phenazine-7,12-dioxide, MPMS: 1-methoxy-5-methylphenazinium methyl sulfate (MPMS), PMS: phenazine methosulfate, PES: phenazine ethosulfate, PHZ: phenazine, OHPHZ: 1-hydroxyphenazine, and PCX: phenazine-1-carboxamide. (B) Current densities as a

1
2
3 function of time for *S. oneidensis* with five different redox mediators. AQS: 9,10-anthraquinone-
4 2-sulfonic acid, AQDS: 9,10-anthraquinone-2,6-disulfonic acid, FMN: flavin mononucleotide,
5 2HNQ: 2-hydroxy-1,4-naphthoquinone, and RF: riboflavin. (C) Scanning electron micrographs
6 showing *S. oneidensis* biofilm formation as a function of redox mediator and time. (D) Current
7 density obtained from *S. oneidensis* with and without outer membrane vesicles (OMVs). Panel A
8 is adapted with permission from ref⁸⁸. Copyright 2021 The Electrochemical Society. Panels B and
9 C are adapted with permission from ref⁸⁹. Copyright 2020 American Chemical Society. Panel D
10 is adapted with permission from ref⁹⁵. Copyright 2019 American Chemical Society.
11
12

13 **Spatiotemporal analysis of metabolites**

14
15 Bacteria are social organisms, so in response to cell-population density and external
16 stimuli, they commonly regulate gene expression and secrete signaling molecules as a means to
17 communicate and coordinate with neighboring organisms, a phenomenon known as quorum
18 sensing or quorum signaling.^{96, 97} Many Gram-negative bacteria secrete N-acyl homoserine
19 lactones (AHL) as the signaling molecule to effect this collective mode of communication. For
20 example, the bioluminescence of *Aliivibrio fischeri* is related to the concentration and action of
21 AHLs.^{98, 99} In one species of opportunistic human pathogenic bacteria, *P. aeruginosa*, four
22 interconnected QS systems, including *las*, *rhl*, *pqs* and *iqs*, with unique signaling molecules
23 associated with each system that are used to coordinate collective activities such as biofilm
24 formation and swarming motility.¹⁰⁰⁻¹⁰² Secreted phenazines, for example, are known to act as
25 virulence factors facilitating the survival of *P. aeruginosa* infections in the host organism.^{103, 104}
26
27 Apart from sensing and quantifying phenazine molecules to track *P. aeruginosa* pathogenesis,
28 spatiotemporal quantification of phenazines can also aid in understanding collective behavior and
29 biofilm formation. *P. aeruginosa* produces a multiplicity of phenazine derivatives, e.g. phenazine-
30 1-carboxylic acid (PCA), 5-methyl-phenazine-1-carboxylic acid (5-MCA), pyocyanin (PYO), and
31 phenazine-1-carboxamide (PCN). Of these, PYO is highly virulent and responsible for both
32 chronic and acute infections.¹⁰⁵⁻¹⁰⁷ Moreover, all of these phenazines are redox-active, undergoing
33
34
35
36
37
38
39
40
41
42
43
44
45
46
47
48
49
50
51
52
53
54
55
56
57
58

1
2
3 reversible proton-coupled electron transfer oxidation/reduction reactions, thus positioning
4
5 electrochemical methods to detect and quantify them.¹⁰⁸⁻¹¹⁰
6
7

8
9 Bard and co-workers used scanning electrochemical microscopy to map the concentration
10
11 of PYO produced in a *P. aeruginosa* biofilm in three-dimensions.¹¹¹ In their approach, a
12
13 microelectrode biased at the oxidation potential of PYO was positioned above the biofilm (**Figure**
14
15 **4A**), and reduced PYO produced by the biofilm diffused to the microelectrode where it could be
16
17 oxidized, with the measured oxidation current being proportional to the PYO concentration. Then,
18
19 the microelectrode was raster-scanned across the biofilm to obtain the electrochemical map shown
20
21 in **Figure 4B**, in which the redox current is proportional to PYO concentration. Moreover, raster
22
23 scanning was done at a different microelectrode-biofilm separations to build a 3D profile of
24
25 secreted PYO. Later, SECM technique was coupled with micro-3D printing (capable of fabricating
26
27 protein-based walls around an individual or small population of bacteria) to understand the
28
29 aggregate size and community-dependent behavior of *P. aeruginosa*,¹¹² revealing that at least 500
30
31 cells per aggregate are required to initiate quorum sensing. By utilizing the wild-type and mutant
32
33 strain aggregates at defined spatial locations, the authors observed at least 2000 cells were required
34
35 to induce quorum sensing in neighboring aggregate positioned 8 μm away. In a complementary
36
37 approach Bellin *et al.*, developed an integrated circuit-based platform for spatial monitoring of
38
39 phenazine produced by a *P. aeruginosa* biofilm.¹¹³ In this structure, an array of electrodes was
40
41 placed under the bacterial colony separated by a thin agar layer. Because the electrodes were
42
43 interrogated in spatially-dependent manner, PYO concentrations were obtained in different
44
45 locations to obtain a spatial map of PYO concentration within the colony. With a spatial resolution
46
47 of 750 μm , they detected higher concentrations of PYO at the colony edges than at the center.
48
49 Interestingly, this result was opposite to the Bard and co-workers' observation, where the redox
50
51
52
53
54
55
56
57
58

1
2
3 current determined by the SECM was higher at the center of the biofilm than the edges. This
4
5 difference could be explained by differences in mass transport mechanisms in the two experimental
6
7 geometries freely diffusing PYO in the SECM map, as opposed to diffusion through an agar matrix
8
9 in the integrated circuit-based platform. The integrated circuit-based platform was later extended
10
11 to image the spatial distribution of multiple phenazine metabolites produced by the *P. aeruginosa*
12
13 PA14 biofilms, finding that while PCA was distributed throughout the colony, 5-MCA and PYO
14
15 were localized near the colony edges.¹¹⁴
16
17
18
19

20 Stevenson and co-workers have also carried out extensive studies of *P. aeruginosa*, based
21
22 on electrochemical detection of phenazines using transparent carbon ultramicroelectrode arrays.^{38,}
23
24 ^{109, 115, 116} For example, they demonstrated temporal tracking of phenazines, showing that PYO
25
26 concentration increases over time in the first 21 h corresponding to the exponential growth of
27
28 bacteria, after which it stabilizes.³⁸ However, 5-MCA, the precursor to PYO, increases until
29
30 intermediate times and decreases later, most likely reflecting the conversion of 5-MCA to PYO.
31
32 In addition, both PYO and 5-MCA production vary slightly as a function of growth medium,
33
34 providing a way to understand the environmental effects on bacterial growth and quorum sensing.
35
36 Using the same approach, they have explored a range of environmental effects on *P. aeruginosa*
37
38 To explore the effect of other bacterial pathogens, *P. aeruginosa* was cultured with other pathogens
39
40 such as *Staphylococcus aureus* and *E. coli* in different growth media, and phenazine production
41
42 was monitored to understand the effect of co-culture.¹⁰⁹ In the presence of *S. aureus*, phenazine
43
44 production was diminished in one growth medium, but not altered in the other. However, the
45
46 presence of *E. coli* in co-culture substantially altered phenazine production independent of growth
47
48 medium. To study the effect of the anti-bacterial agents, these authors targeted the antimicrobial
49
50 properties of Ag⁺ with a specific focus on dynamic effects. Ag⁺ was introduced to bacterial solution
51
52
53
54
55
56
57
58
59
60

grown for 6 h in two different media, and phenazine production decreased substantially within 30 min in both media,¹¹⁶ indicating either inhibition of metabolic process or cell death.

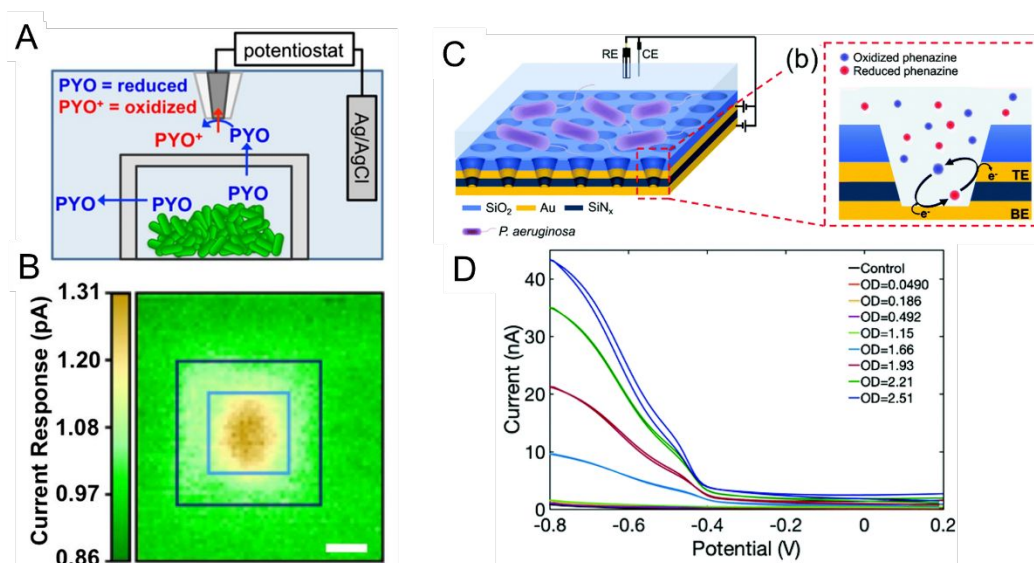


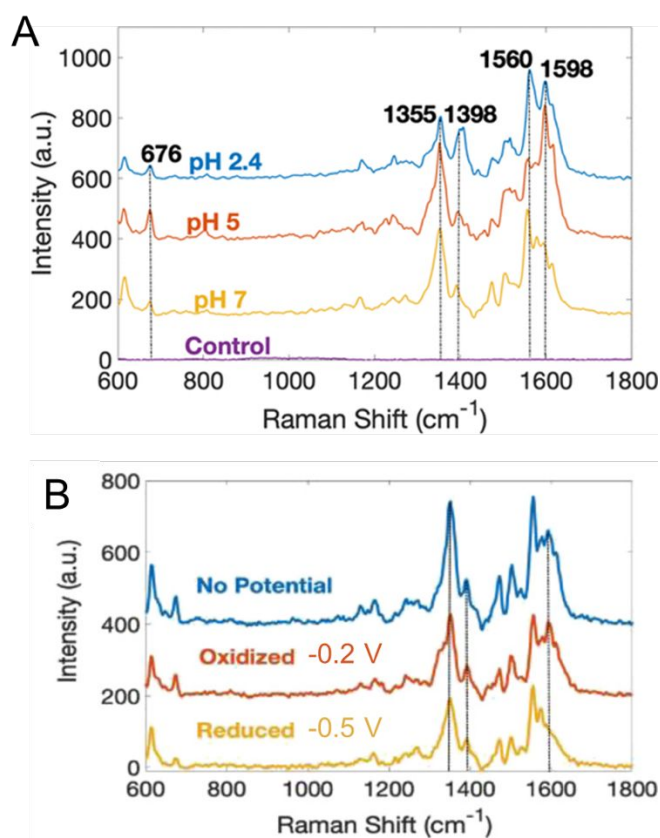
Figure 4. (A) Schematic diagram showing SECM in combination with 3D printed microtrap system for mapping PYO spatial distributions. (B) Electrochemical current maps of PYO secreted by *P. aeruginosa* using the SECM approach of panel A. Scale bar = 10 μm. (C) Left: schematic of dual ring nanopore electrode array (NEA) in contact with *P. aeruginosa*. Right: schematic showing redox cycling of phenazine in NEA. (D) Redox cycling induced cyclic voltammetry of *P. aeruginosa* as a function of optical density (OD). Panels A and B are adapted with permission from ref¹¹². Copyright 2014 National Academy of Sciences. Panel C and D are adapted with permission from ref¹¹⁷. Copyright 2021 The Royal Society of Chemistry.

Since metabolite concentrations are low (< 1 μM) during the initial bacterial growth stages, ultra-sensitive methodologies are needed. To address this challenge, ring-disk nanopore electrode arrays (NEAs), in which the disk electrode at the bottom and the ring electrode at the top of the nanopore is separated by an insulator, were developed in the authors' laboratory.¹¹⁸ Biasing the two electrodes at differing potentials (one oxidizing and one reducing) enables redox cycling with accompanying current amplification thus making ultra-sensitive detection possible. When *P. aeruginosa*-containing solution is added to the top of the NEA devices, the bacteria are excluded from the pores since their diameter is much smaller than the cell size, admitting only metabolites into the nanopore where they undergo redox cycling, thus minimizing biofouling the electrode

1
2
3 surface, as illustrated in **Figure 4C**.¹¹⁷ Redox cycling enhanced voltammetry of PYO produced by
4
5 the *P. aeruginosa* is shown in **Figure 4D**. NEA voltammetry detected phenazines as low as 10 nM
6
7 (PYO) in buffer, and PYO concentrations of 1.5 μM were recovered from the bacterial supernatant.
8
9
10 Apart from ultra-sensitive detection, it is also possible to obtain semi-quantitative estimates of
11
12 families secreted phenazines. Recently, our group extended this work by employing an NEA
13
14 device with a block copolymer (BCP) membrane to selectively determine PCA concentration using
15
16 both electrochemical and surface-enhanced Raman scattering (SERS). Since the BCP membrane
17
18 is both pH- and charge-selective, by adjusting the pH of the bacterial medium above the pKa of
19
20 PCA - but below the pKa of PYO and PCN - it is possible to selectively transport anionic PCA
21
22 into the nanopores for both electrochemical and spectroscopic quantification.¹⁰⁶ In addition, Zor
23
24 and co-workers developed a centrifugal microfluidic lab-on-a-disk platform based on a supported
25
26 liquid membrane (SLM) for extracting, enriching, and detecting hydroxycinnamic acid (pHCA), a
27
28 metabolite produced by *E. coli*.^{119, 120} The platform was constructed with donor and acceptor units
29
30 separated by an SLM acting as a charge selective layer. By tuning the pH of the solution in the
31
32 donor unit, neutral pHCA is able to diffuse through SLM and reach the acceptor unit, while the
33
34 interferants are blocked. This platform detected pHCA concentration as low as 250 μM .
35
36
37
38
39

40
41 With the exception of SECM, most electrochemical methods discussed here can provide
42
43 temporal analysis, but obtaining spatially-dependent information is more challenging.^{38, 109, 115-117,}
44
45 ^{119, 120} Spectroelectrochemistry offers one possible solution to this conundrum. Our group has
46
47 coupled electrochemistry and surface-enhanced Raman spectroscopy (EC-SERS) to map
48
49 phenazines produced by both wild type and mutant *P. aeruginosa* biofilms.¹²¹ Both pH- and
50
51 potential-dependent changes were observed in PYO, as shown in **Figure 5**. Raman band shifts and
52
53 intensity changes were attributed to changes in the electronic structure, especially the central ring
54
55
56
57
58

1
2
3 of PYO induced by proton-coupled electron transfer. In addition, EC-SERS mapping revealed
4 localized PYO deposits approximately the size of *P. aeruginosa* cells, suggesting that PYO
5 secretion remains localized near the cell of origin, at least initially. Thus, EC-SERS is as an elegant
6
7 secretion remains localized near the cell of origin, at least initially. Thus, EC-SERS is as an elegant
8
9 tool for unearthing effect of external conditions on *P. aeruginosa* while also providing spatial
10
11 information about the distribution of secreted metabolites.
12
13
14
15



44 **Figure 5.** Surface-enhanced Raman spectra of PYO as a function of (A) pH, and (B)
45 electrochemical potential. Adapted with permission from ref ¹²¹. Copyright 2019 American
46 Chemical Society.
47
48
49

50 **Single-cell characterization**

51
52 In the last two sections, (spectro)electrochemical characterization of bacteria was considered at the
53
54 ensemble level. Even though the measurements described are enormously powerful in, for
55
56
57
58

1
2
3 example, deciphering EET mechanisms and characterizing the effect of environmental conditions
4
5 on bacterial behavior, with these measurements alone it is not possible to isolate the contribution
6
7 of individual cells to the behavior of the ensemble. On the other hand, characterizing bacteria at
8
9 the single-cell level makes it possible to understand the relationship between cell-to-cell
10
11 heterogeneity and bacterial behavior.¹²² One commonly used method for investigating individual
12
13 cells electrochemically is the single-entity collision or nano-impact methodology,¹²³ in which an
14
15 ultramicroelectrode (UME) with a diameter typically less than 50 μm is used to detect the single
16
17 entities impacting electrode-solution interface. Based on the redox-active nature of the entity these
18
19 events can be classified into either physical blocking or catalytic amplification events. In physical
20
21 blocking events, a small area of the electrode surface is occluded by the impact of a non-redox
22
23 active entity, thereby causing the faradaic current to decrease. Catalytic amplification events, on
24
25 the other hand, occurs when a redox-active catalytic entity contacts the UME under conditions
26
27 where no electrochemical reaction would otherwise occur, thus producing an increase in current.
28
29 Sepunaru *et al.* and Frkonja-Kuczyn *et al.* detected *E. coli* by decorating them with Ag
30
31 nanoparticles (NPs) and poisoning the UME at a potential to oxidize Ag, so the collision of single
32
33 AgNP-decorated *E. coli* cells would be signaled by a transient increase in faradaic current resulting
34
35 from the oxidation of the AgNPs.^{124, 125} While AgNP labeling is effective, the anti-microbial
36
37 property of Ag can potentially kill the cells.¹²⁶ To overcome this issue, Lee *et al.* used the blocking
38
39 approach to detect *E. coli*, using the collision of *E. coli* at a UME to impede the oxidation of
40
41 ferrocyanide, as shown in **Figure 6A**, top panel.¹²⁷ A similar response was observed by Lebègue
42
43 *et al.* for single *S. oneidensis* cells on a carbon UME.¹²⁸ Ronspees and Thorgaard incorporated a
44
45 fluorescence microscope in the blocking experiment to simultaneously track the attachment and
46
47 movement of bacterial cells on the UME surface.¹²⁹ In their experiment, *E. coli* showed a step
48
49
50
51
52
53
54
55
56
57
58
59
60

current decrease as observed by other groups, however they observed that *B. subtilis* produced a transient current blockage. Fluorescence imaging confirmed that the step response is associated with the attachment of bacterial cells (**Figures 6B and 6C**), while the transient response corresponds to short-lived cell attachment. Thus, spectroelectrochemical studies events can further elucidate the dynamics of single bacterial cell collision events at UMEs.

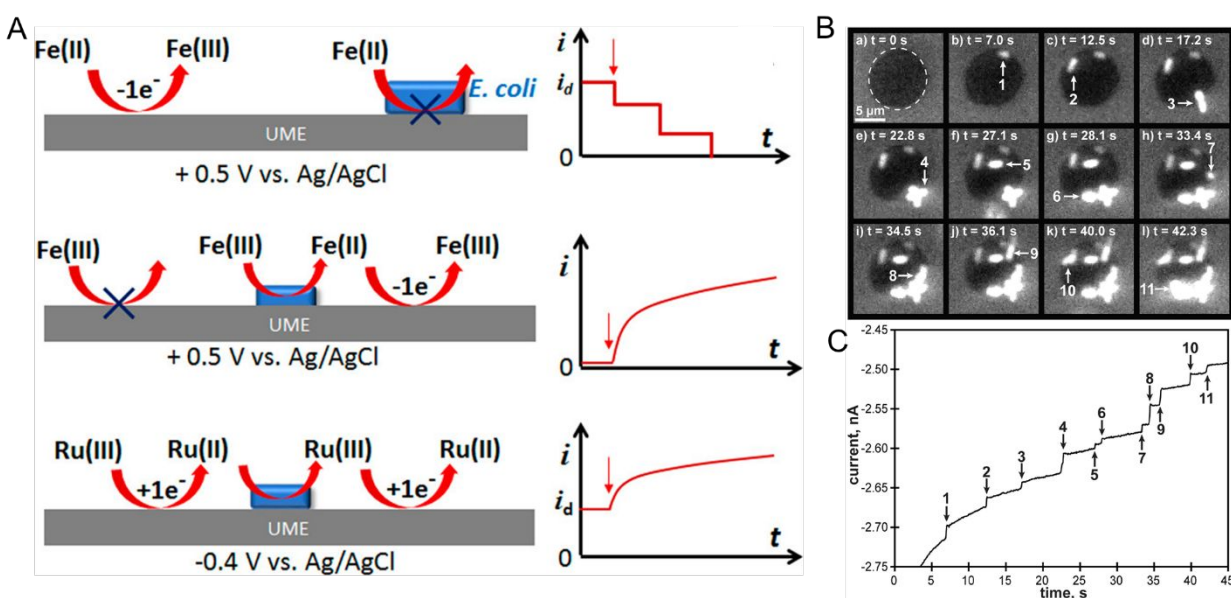


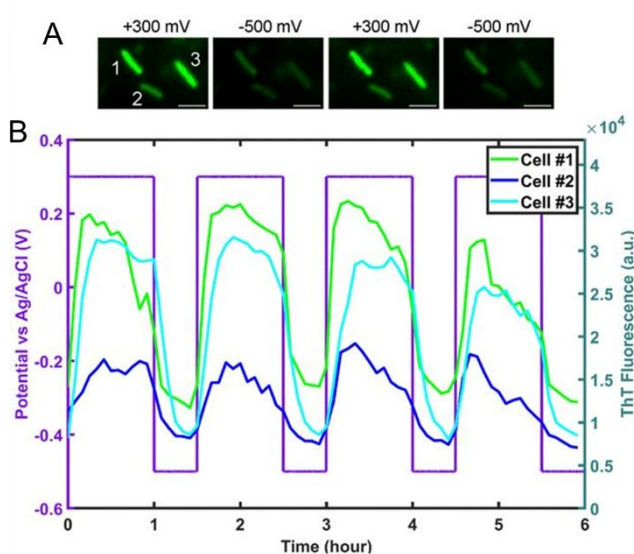
Figure 6. (A) Different ways of detecting bacteria-electrode collisions along with their current-time responses. Top panel: bacterial cell blocking the UME electroactive area; Middle panel: bacterial cell catalyzing reduction; Bottom panel: regeneration of redox species by bacterial cell. (B) Time-lapse fluorescence images showing *E. coli* attaching to the UME surface. (C) Current-time trace corresponding to panel B. Panel A is adapted with permission from ref ¹³⁰. Copyright 2018 American Chemical Society. Panels B and C are adapted with permission from ref ¹²⁹. Copyright 2018 Elsevier Ltd.

A disadvantage of the blocking approach is that it is useful only for detecting the bacteria; it cannot be used to understand their redox activity. However, by taking advantage of the redox-active nature of *E. coli*, Gao *et al.*, evaluated the redox activity of a single bacterial cell.¹³⁰ As shown in **Figure 6A**, middle panel, *E. coli* reduces ferricyanide to ferrocyanide, which in turn can be re-oxidized back to ferricyanide at the UME. Thus, the measured current is directly proportional to

1
2
3 the reduction efficiency of individual *E. coli* cells. Alternatively, reduced (oxidized) species
4 generated at the UME can be oxidized (reduced) by the bacterial cell attached to the UME (**Figure**
5 **6A**, bottom panel). The regeneration of species by the bacterial cell increases the overall current
6 providing an efficient way to understand microbial redox activity. Furthermore, this approach has
7 been extended to assess the effect of antimicrobial agents such as cobalt ions and colistin. Compton
8 and co-workers used N,N,N',N'-tetramethyl-para-phenylene-diamine (TMPD) as a redox mediator
9 to characterize the behavior of single *E. coli* cells, exploiting the fact that cytochrome c oxidase
10 expressed in *E. coli* oxidizes TMPD to TMPD^{••} which gets regenerated (reduced) at the UME
11 making it possible to assess both redox activity and cell viability.¹³¹

12 Spectroelectrochemical approaches have also been employed to reveal variation in EET at
13 the single entity level. El-Naggar and co-workers used Thioflavin T, a fluorescent cationic dye,
14 and Nernstian membrane potential indicator to study the dynamics of *S. oneidensis* MR-1
15 membrane potential during potential-induced EET.¹³² Application of a positive external potential
16 (+0.3 V) was observed to result in a negative EET membrane potential, leading to accumulation
17 of positive Thioflavin T in the membrane, thus increasing fluorescence, as shown in **Figure 7A**,
18 first panel. The reverse process occurred when a negative external potential (-0.5 V) was applied
19 (**Figure 7A**, second panel). The potential-dependent fluorescence was followed over three
20 consecutive potential step cycles. Moreover, the potential- and time-dependent fluorescence
21 intensity traces for three different cells shown in **Figure 7B** indicate considerable cell-to-cell
22 variation, revealing heterogeneity in EET. Recent work from our laboratory in collaboration with
23 Willets used a coupled fluorescence and electrochemical approach to probe direct EET in
24 *Myxococcus xanthus*, a soil-dwelling bacterium important in the degradation of woody plant
25 materials.¹³³ Instead of adding external flavins, the potential dependent fluorescence dynamics was

1
2
3 tracked using intrinsic membrane-associated flavoproteins, which contain flavin molecules such
4
5 flavin mononucleotide (FMN) and flavin adenine dinucleotide (FAD), whose fluorescence
6
7 changes based on redox state, *i.e.* fluorescent and non-fluorescent in the oxidized and reduced
8
9 forms, respectively.¹³⁴ The observation of a non-canonical potential response from bacteria led to
10
11 a detailed investigation of the potential, concentration, and irradiance dependence of the model
12
13 electrofluorogenic compound FMN molecule, showing that the carrier dynamics of the ITO
14
15 substrate play an important role in determining the potential-dependent fluorescence response, thus
16
17 emphasizing the importance of the electrode in spectroelectrochemical experiments, especially at
18
19 the single-cell level.
20
21
22



23
24
25
26
27
28
29
30
31
32
33
34
35
36
37
38
39
40
41
42 **Figure 7.** (A) Fluorescence images of *S. oneidensis* with thioflavin T obtained as a function of
43 electrochemical potential. (B) Electrochemical potential- and fluorescence intensity-time traces
44 for three individual cells marked in panel A. Adapted with permission from ref. ¹³². 2020 National
45 Academy of Sciences.
46

47 48 49 **Conclusion and Outlook**

50
51 This review addressed recent advances in the use of electrochemical and
52
53 spectroelectrochemical approaches to characterize bacterial systems in three broad areas. In
54
55 microbial electron transfer, electrochemical and spectroelectrochemical techniques have been used
56
57
58

1
2
3 to obtain mechanistic understanding of direct EET. The effect of redox mediator properties on
4
5 EET and biofilm formation, which facilitate efficiency of bioelectrochemical systems, was also
6
7 discussed. Apart from using spectroelectrochemical techniques to obtain more accurate
8
9 mechanistic insight on EET, future research direction can productively focus on understanding the
10
11 role of external factors, such as irradiation, on EET and gene expression. Further, *in situ*
12
13 electrochemical inactivation and cell lysis could be used to analyze altered gene expression and
14
15 correlate these with EET responses.^{135, 136}
16
17
18
19

20 Second, approaches to reveal the spatiotemporal distributions of secreted factors, *e.g.*
21
22 metabolites, were highlighted. SECM and integrated electrochemical chip-based detection provide
23
24 three- and two-dimensional spatial distribution of metabolites, respectively. Carbon-based
25
26 ultramicroelectrode and nanopore-electrode arrays have been used to achieve ultra-sensitive
27
28 detection of metabolites enabling the development of electrochemical sensors for pathogenic
29
30 bacteria. Moreover, EC-SERS is able to visualize metabolite spatial distributions as a function of
31
32 changing environmental conditions. Given that chemical identity and concentration of secreted
33
34 metabolites are a sensitive function of the environment, efforts to culture bacteria on miniaturized
35
36 scales coupled to dynamic *in situ* strategies to alter the environment coupled to the metabolites
37
38 measurement using spectroelectrochemistry with high spatial and temporal resolution would
39
40 appear to hold much promise.
41
42
43
44
45

46 In the final section, we described electrochemical collision-based techniques for detecting
47
48 single bacteria cells and measuring EET at the single-cell level. Further, fluorescence microscopy
49
50 coupled with electrochemistry was found to be useful for high-throughput measurement of EETs
51
52 in individual cells and to uncover cell-to-cell heterogeneity in EET kinetics. Future studies that
53
54 can exploit the capability to isolate or compartmentalize individual bacteria in defined locations
55
56
57
58

1
2
3 and study them using spectroelectrochemistry would enable us to understand not only
4 heterogeneity between the cells but also to realize their intercellular behavior under well-defined
5 conditions. Moreover, owing to the emergence of powerful new electrochemical imaging
6 approaches, such as SECM, scanning ion conductance microscopy (SICM) scanning
7 electrochemical cell microscopy (SECCM), and scanning photoelectrochemical microscopy
8 (SPECM), it is possible to measure pH, surface charge, intracellular substances, membrane
9 proteins, mechanical properties, and redox mediator transport by mapping them at the single-cell
10 level.¹³⁷⁻¹³⁹ Additionally, advances in optical imaging, such as super-resolution,¹⁴⁰ structured
11 illumination,¹⁴¹ appear more ripe for combining with electrochemistry to achieve unprecedented
12 advances in understanding behavior of bacteria and bacterial assemblies.
13
14
15
16
17
18
19
20
21
22
23
24
25

26 **Conflicts of interest**

27
28
29 The authors declare no conflict of interest.
30
31

32 **Acknowledgments**

33
34
35 The authors would like to acknowledge financial support from the following agencies for
36 work described here from their laboratory: the Department of Energy Office of Science (Grant
37 DE-SC0019312), the National Science Foundation (CHE-1904196), and the National Institutes of
38 Health (R01 AI113219-06).
39
40
41
42
43
44

45 **References:**

- 46
47 1. R. Franco-Duarte, L. Černáková, S. Kadam, K. S. Kaushik, B. Salehi, A. Bevilacqua, M.
48 R. Corbo, H. Antolak, K. Dybka-Stępień, M. Leszczewicz, S. Relison Tintino, V. C.
49 Alexandrino de Souza, J. Sharifi-Rad, H. D. Melo Coutinho, N. Martins and C. F.
50 Rodrigues, *Microorganisms*, 2019, **7**, 130.
51
52
53
54
55
56
57
58

- 1
2
3 2. Q. Zhang, M. Raoof, Y. Chen, Y. Sumi, T. Sursal, W. Junger, K. Brohi, K. Itagaki and C.
4
5 J. Hauser, *Nature*, 2010, **464**, 104-U115.
6
7
- 8
9 3. J. M. Lorenzo, P. E. Munekata, R. Dominguez, M. Pateiro, J. A. Saraiva and D. Franco,
10
11 in *Innovative Technologies for Food Preservation*, eds. F. J. Barba, A. S. Sant'Ana, V.
12
13 Orlien and M. Koubaa, Academic Press, 2018, DOI: [https://doi.org/10.1016/B978-0-12-](https://doi.org/10.1016/B978-0-12-811031-7.00003-0)
14
15 [811031-7.00003-0](https://doi.org/10.1016/B978-0-12-811031-7.00003-0), pp. 53-107.
16
17
- 18
19 4. L. Gram, L. Ravn, M. Rasch, J. B. Bruhn, A. B. Christensen and M. Givskov,
20
21 *International Journal of Food Microbiology*, 2002, **78**, 79-97.
22
23
- 24
25 5. M. E. J. Woolhouse and S. Gowtage-Sequeria, *Emerging Infectious Disease journal*,
26
27 2005, **11**, 1842.
28
29
- 30
31 6. K. W. McConnell, J. E. McDunn, A. T. Clark, W. M. Dunne, D. J. Dixon, I. R. Turnbull,
32
33 P. J. Dipasco, W. F. Osberghaus, B. Sherman, J. R. Martin, M. J. Walter, J. P. Cobb, T.
34
35 G. Buchman, R. S. Hotchkiss and C. M. Coopersmith, *Critical care medicine*, 2010, **38**,
36
37 223-241.
38
39
- 40
41 7. P. Martens, S. W. Worm, B. Lundgren, H. B. Konradsen and T. Benfield, *BMC Infectious*
42
43 *Diseases*, 2004, **4**, 21.
44
45
- 46
47 8. D. Emerson, L. Agulto, H. Liu and L. Liu, *BioScience*, 2008, **58**, 925-936.
48
49
- 50
51 9. A. Ahmed, J. V. Rushworth, N. A. Hirst and P. A. Millner, *Clinical Microbiology*
52
53 *Reviews*, 2014, **27**, 631-646.
54
55
56
57
58

- 1
2
3 10. O. Lazcka, F. J. Del Campo and F. X. Munoz, *Biosensors & Bioelectronics*, 2007, **22**,
4
5 1205-1217.
6
7
- 8
9 11. J. Hu and P. W. Bohn, *J. Anal. Test.*, 2017, **1**, 1-17.
10
- 11
12 12. R. Karlsson, L. Gonzales-Siles, M. Gomila, A. Busquets, F. Salvà-Serra, D. Jaén-
13
14 Luchoro, H. E. Jakobsson, A. Karlsson, F. Boulund, E. Kristiansson and E. R. B. Moore,
15
16 *PloS one*, 2018, **13**, e0208804-e0208804.
17
18
- 19
20 13. S. A. Barghouthi, *Indian Journal of Microbiology*, 2011, **51**, 430-444.
21
22
- 23
24 14. P. Athamanolap, K. Hsieh, L. Chen, S. Yang and T.-H. Wang, *Analytical Chemistry*,
25
26 2017, **89**, 11529-11536.
27
28
- 29
30 15. L. Zhu, Y. Zhang, P. He, Y. Zhang and Q. Wang, *Journal of Chromatography B*, 2018,
31
32 **1093-1094**, 141-146.
33
- 34
35 16. F. Nomura, S. Tsuchida, S. Murata, M. Satoh and K. Matsushita, *Clinical Proteomics*,
36
37 2020, **17**, 14.
38
39
- 40
41 17. B. Rodríguez-Sánchez and M. Oviaño, in *Application and Integration of Omics-powered*
42
43 *Diagnostics in Clinical and Public Health Microbiology*, eds. J. Moran-Gilad and Y.
44
45 Yagel, Springer International Publishing, Cham, 2021, DOI: 10.1007/978-3-030-62155-
46
47 1_10, pp. 175-189.
48
49
- 50
51 18. C. R. Cox and K. J. Voorhees, Dordrecht, 2014.
52
- 53
54 19. P. Rubbens, R. Props, N. Boon and W. Waegeman, *PLoS One*, 2017, **12**, e0169754.
55
56
57
58

- 1
2
3 20. L. X. Coggins, I. Larma, A. Hinchliffe, R. Props and A. Ghadouani, *Water Research*,
4 2020, **169**, 115243.
5
6
7
8
9 21. Y. Shen, Y. Zhang, Z. F. Gao, Y. Ye, Q. Wu, H.-Y. Chen and J.-J. Xu, *Nano Today*,
10 2021, **38**, 101121.
11
12
13
14 22. A. Qureshi and J. H. Niazi, *Analyst*, 2020, **145**, 7825-7848.
15
16
17 23. Y. Xu, M. M. Hassan, A. S. Sharma, H. Li and Q. Chen, *Critical Reviews in Food*
18 *Science and Nutrition*, 2021, DOI: 10.1080/10408398.2021.1950117, 1-19.
19
20
21
22
23 24. S. A. Strola, J.-C. Baritoux, E. Schultz, A. C. Simon, C. Allier, I. Espagnon, D. Jary and
24 J.-M. Dinten, *Journal of Biomedical Optics*, 2014, **19**, 111610.
25
26
27
28
29 25. J. P. Harrison and D. Berry, *Frontiers in microbiology*, 2017, **8**, 675-675.
30
31
32 26. M. Harz, P. Rösch and J. Popp, *Cytometry Part A*, 2009, **75A**, 104-113.
33
34
35 27. Y. Chen, C. Zou, M. Mastalerz, S. Hu, C. Gasaway and X. Tao, *International journal of*
36 *molecular sciences*, 2015, **16**, 30223-30250.
37
38
39
40
41 28. T. Cao, J. V. Sweedler, P. W. Bohn, J. D. Shrout and C. D. Ellermeier, *mSphere*, 2020, **5**,
42 e00426-00420.
43
44
45
46 29. T. Cao, A. A. Weaver, S. Baek, J. Jia, J. D. Shrout and P. W. Bohn, *The Journal of*
47 *Chemical Physics*, 2021, **154**, 204201.
48
49
50
51
52 30. H.-Y. N. Holman, R. Miles, Z. Hao, E. Wozzi, L. M. Anderson and H. Yang, *Analytical*
53 *Chemistry*, 2009, **81**, 8564-8570.
54
55
56
57
58

- 1
2
3 31. S. Kuss, H. M. A. Amin and R. G. Compton, *Chemistry – An Asian Journal*, 2018, **13**,
4 2758-2769.
5
6
7
8
9 32. O. Simoska and K. J. Stevenson, *Analyst*, 2019, **144**, 6461-6478.
10
11
12 33. M. C. Potter and A. D. Waller, *Proceedings of the Royal Society of London. Series B,*
13 *Containing Papers of a Biological Character*, 1911, **84**, 260-276.
14
15
16
17 34. R. Y. A. Hassan, F. Febbraio and S. Andreescu, *Sensors*, 2021, **21**, 1279.
18
19
20
21 35. F. Kracke, I. Vassilev and J. O. Krömer, *Frontiers in microbiology*, 2015, **6**, 575-575.
22
23
24 36. K.-M. Moon, H.-R. Cho, M.-H. Lee, S.-K. Shin and S.-C. Koh, *Metals and Materials*
25 *International*, 2007, **13**, 211.
26
27
28
29
30 37. K.-Y. Chan, L.-C. Xu and H. H. P. Fang, *Environmental Science & Technology*, 2002,
31 **36**, 1720-1727.
32
33
34
35 38. O. Simoska, M. Sans, M. D. Fitzpatrick, C. M. Crittenden, L. S. Eberlin, J. B. Shear and
36 K. J. Stevenson, *ACS Sensors*, 2019, **4**, 170-179.
37
38
39
40
41 39. Y. Qiao, C. M. Li, S.-J. Bao, Z. Lu and Y. Hong, *Chemical Communications*, 2008, DOI:
42 10.1039/B719955D, 1290-1292.
43
44
45
46
47 40. D. Millo, *Biochemical Society Transactions*, 2012, **40**, 1284-1290.
48
49
50 41. Y. Zhai, Z. Zhu, S. Zhou, C. Zhu and S. Dong, *Nanoscale*, 2018, **10**, 3089-3111.
51
52
53 42. M. Sezer, D. Millo, I. M. Weidinger, I. Zebger and P. Hildebrandt, *IUBMB Life*, 2012,
54 **64**, 455-464.
55
56
57
58

- 1
2
3 43. D. Millo, A. Bonifacio, M. R. Moncelli, V. Sergo, C. Gooijer and G. van der Zwan,
4
5 *Colloids and Surfaces B: Biointerfaces*, 2010, **81**, 212-216.
6
7
8
9 44. J. P. Busalmen, A. Esteve-Núñez, A. Berná and J. M. Feliu, *Angewandte Chemie*
10
11 *International Edition*, 2008, **47**, 4874-4877.
12
13
14 45. X. B. Liu, L. Shi and J. D. Gu, *Biotechnology Advances*, 2018, **36**, 1815-1827.
15
16
17
18 46. B. E. Logan, R. Rossi, A. Ragab and P. E. Saikaly, *Nature Reviews Microbiology*, 2019,
19
20 **17**, 307-319.
21
22
23 47. A. J. Slate, K. A. Whitehead, D. A. C. Brownson and C. E. Banks, *Renewable &*
24
25 *Sustainable Energy Reviews*, 2019, **101**, 60-81.
26
27
28
29 48. X. X. Xiao, H. Q. Xia, R. R. Wu, L. Bai, L. Yan, E. Magner, S. Cosnier, E. Lojou, Z. G.
30
31 Zhu and A. H. Liu, *Chemical Reviews*, 2019, **119**, 9509-9558.
32
33
34 49. H. Chen, O. Simoska, K. Lim, M. Grattieri, M. Yuan, F. Dong, Y. S. Lee, K. Beaver, S.
35
36 Weliwatte, E. M. Gaffney and S. D. Minteer, *Chemical Reviews*, 2020, **120**, 12903-
37
38 12993.
39
40
41
42 50. E. Zhou, Y. Lekbach, T. Gu and D. Xu, *Current Opinion in Electrochemistry*, 2021, DOI:
43
44 <https://doi.org/10.1016/j.coelec.2021.100830>, 100830.
45
46
47
48 51. S. N. Victoria, A. Sharma and R. Manivannan, *Journal of the Indian Chemical Society*,
49
50 2021, **98**, 100083.
51
52
53
54 52. G. Pankratova, L. Hederstedt and L. Gorton, *Analytica Chimica Acta*, 2019, **1076**, 32-47.
55
56
57
58

- 1
2
3 53. R. L. Heydorn, C. Engel, R. Krull and K. Dohnt, *ChemBioEng Reviews*, 2020, **7**, 4-17.
4
5
6
7 54. B. J. Little, D. J. Blackwood, J. Hinks, F. M. Lauro, E. Marsili, A. Okamoto, S. A. Rice,
8
9 S. A. Wade and H. C. Flemming, *Corrosion Science*, 2020, **170**, 108641.
10
11
12 55. Y. Ma, Y. Zhang, R. Zhang, F. Guan, B. Hou and J. Duan, *Applied Microbiology and*
13
14 *Biotechnology*, 2020, **104**, 515-525.
15
16
17 56. F. McEachern, E. Harvey and G. Merle, *Biotechnology Journal*, 2020, **15**, 2000140.
18
19
20
21 57. Y. L. L Chen, X Tian, F Zhao, *Progress in chemistry*, 2020, **32**, 1557-1563.
22
23
24 58. B. E. Logan, R. Rossi, A. a. Ragab and P. E. Saikaly, *Nature Reviews Microbiology*,
25
26 2019, **17**, 307-319.
27
28
29
30 59. K. P. Nevin, H. Richter, S. F. Covalla, J. P. Johnson, T. L. Woodard, A. L. Orloff, H. Jia,
31
32 M. Zhang and D. R. Lovley, *Environmental Microbiology*, 2008, **10**, 2505-2514.
33
34
35 60. N. S. Malvankar, M. T. Tuominen and D. R. Lovley, *Energy & Environmental Science*,
36
37 2012, **5**, 8651-8659.
38
39
40
41 61. D. R. Bond, S. M. Strycharz-Glaven, L. M. Tender and C. I. Torres, *ChemSusChem*,
42
43 2012, **5**, 1099-1105.
44
45
46 62. A. Jain, G. Gazzola, A. Panzera, M. Zanoni and E. Marsili, *Electrochimica Acta*, 2011,
47
48 **56**, 10776-10785.
49
50
51
52 63. R. M. Snider, S. M. Strycharz-Glaven, S. D. Tsoi, J. S. Erickson and L. M. Tender,
53
54 *Proceedings of the National Academy of Sciences*, 2012, **109**, 15467-15472.
55
56
57
58

- 1
2
3 64. G. D. Schrott, P. S. Bonanni and J. P. Busalmen, *Electrochimica Acta*, 2019, **303**, 176-
4 182.
5
6
7
8
9 65. A. Krige, K. Ramser, M. Sjöblom, P. Christakopoulos, U. Rova and R. M. Kelly, *Applied*
10 *and Environmental Microbiology*, 2020, **86**, e01535-01520.
11
12
13
14 66. N. Heidary, N. Kornienko, S. Kalathil, X. Fang, K. H. Ly, H. F. Greer and E. Reisner,
15 *Journal of the American Chemical Society*, 2020, **142**, 5194-5203.
16
17
18
19
20 67. Y. Yi, T. Zhao, Y. Zang, B. Xie and H. Liu, *Electrochemistry Communications*, 2021,
21 **124**, 106966.
22
23
24
25 68. X. Liu, J. Zhan, L. Liu, F. Gan, J. Ye, K. H. Neilson, C. Rensing and S. Zhou,
26 *Environmental Science & Technology*, 2021, **55**, 10142-10151.
27
28
29
30
31 69. G. A. Huerta-Miranda, A. I. Arroyo-Escoto, X. Burgos, K. Juárez and M. Miranda-
32 Hernández, *Bioelectrochemistry*, 2019, **127**, 145-153.
33
34
35
36
37 70. B. Zhang, H.-Y. Cheng and A. Wang, *Bioelectrochemistry*, 2021, **138**, 107683.
38
39
40
41 71. N. M. Tefft and M. A. TerAvest, *ACS Synthetic Biology*, 2019, **8**, 1590-1600.
42
43
44 72. Y. Yang, Z. Wang, C. Gan, L. H. Klausen, R. Bonn e, G. Kong, D. Luo, M. Meert, C.
45 Zhu, G. Sun, J. Guo, Y. Ma, J. T. Bjerg, J. Manca, M. Xu, L. P. Nielsen and M. Dong,
46 *Nature Communications*, 2021, **12**, 1709.
47
48
49
50
51 73. W. Wang, Y. Du, S. Yang, X. Du, M. Li, B. Lin, J. Zhou, L. Lin, Y. Song, J. Li, X. Zuo
52 and C. Yang, *Analytical Chemistry*, 2019, **91**, 12138-12141.
53
54
55
56
57
58

- 1
2
3 74. D. Naradasu, A. Guionet, T. Okinaga, T. Nishihara and A. Okamoto, *ChemElectroChem*,
4 2020, **7**, 2012-2019.
5
6
7
8
9 75. S. Werwinski, J. A. Wharton, M. Nie and K. R. Stokes, *ACS Applied Materials &*
10 *Interfaces*, 2021, **13**, 31393-31405.
11
12
13
14 76. A. A. Karbelkar, A. R. Rowe and M. Y. El-Naggar, *Electrochimica Acta*, 2019, **324**,
15 134838.
16
17
18
19
20 77. I. Brand and B. Khairalla, *Faraday Discussions*, 2020, DOI: 10.1039/D0FD00039F.
21
22
23 78. B. Abada, S. Boumerfeg, A. Haddad and M. Etienne, *Journal of The Electrochemical*
24 *Society*, 2020, **167**, 135502.
25
26
27
28
29 79. H. P. Bennetto, J. L. Stirling, K. Tanaka and C. A. Vega, *Biotechnology and*
30 *Bioengineering*, 1983, **25**, 559-568.
31
32
33
34 80. T. W. Seviour and J. Hinks, *Critical Reviews in Biotechnology*, 2018, **38**, 634-646.
35
36
37
38 81. X. Liu, L. Shi and J.-D. Gu, *Biotechnology Advances*, 2018, **36**, 1815-1827.
39
40
41 82. D. H. Park and J. G. Zeikus, *Applied and Environmental Microbiology*, 2000, **66**, 1292-
42 1297.
43
44
45
46 83. S.-L. Li, Y.-J. Wang, Y.-C. Chen, S.-M. Liu and C.-P. Yu, *Frontiers in Microbiology*,
47 2019, **10**.
48
49
50
51
52 84. M. Grattieri, Z. Rhodes, D. P. Hickey, K. Beaver and S. D. Minter, *ACS Catalysis*, 2019,
53 **9**, 867-873.
54
55
56
57
58

- 1
2
3 85. K. Rabaey, N. Boon, M. Höfte and W. Verstraete, *Environmental Science & Technology*,
4 2005, **39**, 3401-3408.
5
6
7
8
9 86. E. VanArsdale, J. Pitzer, G. F. Payne and W. E. Bentley, *iScience*, 2020, **23**, 101545.
10
11
12 87. T. Tschirhart, E. Kim, R. McKay, H. Ueda, H.-C. Wu, A. E. Pottash, A. Zargar, A.
13 Negrete, J. Shiloach, G. F. Payne and W. E. Bentley, *Nature Communications*, 2017, **8**,
14 14030.
15
16
17
18
19
20 88. O. Simoska, E. M. Gaffney, K. Lim, K. Beaver and S. D. Minter, *Journal of The*
21 *Electrochemical Society*, 2021, **168**, 025503.
22
23
24
25
26 89. Y. Wu, X. Luo, B. Qin, F. Li, M. M. Häggblom and T. Liu, *Environmental Science &*
27 *Technology*, 2020, **54**, 7217-7225.
28
29
30
31 90. E. Marsili, D. B. Baron, I. D. Shikhare, D. Coursolle, J. A. Gralnick and D. R. Bond,
32 *Proceedings of the National Academy of Sciences*, 2008, **105**, 3968-3973.
33
34
35
36
37 91. R. Starwalt-Lee, M. Y. El-Naggar, D. R. Bond and J. A. Gralnick, *Molecular*
38 *Microbiology*, 2021, **115**, 1069-1079.
39
40
41
42 92. T. Tian, X. Fan, M. Feng, L. Su, W. Zhang, H. Chi and D. Fu, *RSC Advances*, 2019, **9**,
43 40903-40909.
44
45
46
47
48 93. D. M. Gurumurthy, R. N. Bharagava, A. Kumar, B. Singh, M. Ashfaq, G. D. Saratale and
49 S. I. Mulla, *Microbiological Research*, 2019, **229**, 126324.
50
51
52
53 94. J. Guo, G. Yang, Z. Zhuang, Q. Mai and L. Zhuang, *Science of The Total Environment*,
54 2021, **797**, 149207.
55
56
57
58

- 1
2
3 95. X. Liu, X. Jing, Y. Ye, J. Zhan, J. Ye and S. Zhou, *Environmental Science & Technology*
4 *Letters*, 2020, **7**, 27-34.
5
6
7
8
9 96. A. Sharma, P. Singh, B. K. Sarmah and S. P. Nandi, *Research in Microbiology*, 2020,
10 **171**, 159-164.
11
12
13
14 97. O. P. Duddy and B. L. Bassler, *PLOS Pathogens*, 2021, **17**, e1009074.
15
16
17
18 98. S. T. Rutherford and B. L. Bassler, *Cold Spring Harbor perspectives in medicine*, 2012,
19 **2**, a012427.
20
21
22
23 99. M. Molnár, É. Fenyvesi, Z. Berkl, I. Németh, I. Fekete-Kertész, R. Márton, E. Vaszita, E.
24 Varga, D. Ujj and L. Szente, *International Journal of Pharmaceutics*, 2021, **594**, 120150.
25
26
27
28
29 100. S. Mukherjee and B. Bassler, *Nat. Rev. Microbiol.*, 2019, **17**, 371-382.
30
31
32 101. J. Shrouf, T. Tolker-Nielsen, M. Givskov and M. Parsek, *MRS Bull.*, 2011, **36**, 367-373.
33
34
35
36 102. K. Brindhadevi, F. LewisOscar, E. Mylonakis, S. Shanmugam, T. N. Verma and A.
37 Pugazhendhi, *Process Biochemistry*, 2020, **96**, 49-57.
38
39
40
41 103. A. J. Sabat, D. Pantano, V. Akkerboom, E. Bathoorn and A. W. Friedrich, *Biological*
42 *Chemistry*, 2021, DOI: doi:10.1515/hsz-2021-0243.
43
44
45
46
47 104. L. Vilaplana and M. P. Marco, *Analytical and Bioanalytical Chemistry*, 2020, **412**, 5897-
48 5912.
49
50
51
52 105. M. Z. El-Fouly, A. M. Sharaf, A. A. M. Shahin, H. A. El-Bialy and A. M. A. Omara,
53 *Journal of Radiation Research and Applied Sciences*, 2015, **8**, 36-48.
54
55
56
57
58

- 1
2
3 106. J. Jia, S.-R. Kwon, S. Baek, V. Sundaresan, T. Cao, A. R. Cutri, K. Fu, B. Roberts, J. D.
4
5 Shrouf and P. W. Bohn, *Analytical Chemistry*, 2021, DOI:
6
7 10.1021/acs.analchem.1c02998.
8
9
10
11 107. J. Oziat, T. Cohu, S. Elsen, M. Gougis, G. G. Malliaras and P. Mailley,
12
13 *Bioelectrochemistry*, 2021, **140**, 107747.
14
15
16 108. A. Buzid, F. Shang, F. J. Reen, E. Ó. Muimhneacháin, S. L. Clarke, L. Zhou, J. H. T.
17
18 Luong, F. O’Gara, G. P. McGlacken and J. D. Glennon, *Scientific Reports*, 2016, **6**,
19
20 30001.
21
22
23
24 109. O. Simoska, M. Sans, L. S. Eberlin, J. B. Shear and K. J. Stevenson, *Biosensors and*
25
26 *Bioelectronics*, 2019, **142**, 111538.
27
28
29
30 110. F. A. a. Alatraktchi, W. E. Svendsen and S. Molin, *Sensors*, 2020, **20**, 5218.
31
32
33 111. D. Koley, M. M. Ramsey, A. J. Bard and M. Whiteley, *Proceedings of the National*
34
35 *Academy of Sciences*, 2011, **108**, 19996.
36
37
38
39 112. J. L. Connell, J. Kim, J. B. Shear, A. J. Bard and M. Whiteley, *Proceedings of the*
40
41 *National Academy of Sciences*, 2014, **111**, 18255.
42
43
44 113. D. L. Bellin, H. Sakhtah, J. K. Rosenstein, P. M. Levine, J. Thimot, K. Emmett, L. E. P.
45
46 Dietrich and K. L. Shepard, *Nature Communications*, 2014, **5**, 3256.
47
48
49
50 114. D. L. Bellin, H. Sakhtah, Y. Zhang, A. Price-Whelan, L. E. P. Dietrich and K. L.
51
52 Shepard, *Nature Communications*, 2016, **7**, 10535.
53
54
55
56
57
58

- 1
2
3 115. J. Elliott, O. Simoska, S. Karasik, J. B. Shear and K. J. Stevenson, *Analytical Chemistry*,
4 2017, **89**, 6285-6289.
5
6
7
8
9 116. O. Simoska, J. Duay and K. J. Stevenson, *ACS Sensors*, 2020, **5**, 3547-3557.
10
11
12 117. H. Do, S.-R. Kwon, S. Baek, C. S. Madukoma, M. K. Smiley, L. E. Dietrich, J. D. Shrout
13 and P. W. Bohn, *Analyst*, 2021, **146**, 1346-1354.
14
15
16
17 118. K. Fu, S.-R. Kwon, D. Han and P. W. Bohn, *Accounts of Chemical Research*, 2020, **53**,
18 719-728.
19
20
21
22
23 119. K. Sanger, K. Zór, C. Bille Jendresen, A. Heiskanen, L. Amato, A. Toftgaard Nielsen and
24 A. Boisen, *Sensors and Actuators B: Chemical*, 2017, **253**, 999-1005.
25
26
27
28 120. S. Z. Andreasen, K. Sanger, C. B. Jendresen, A. T. Nielsen, J. Emnéus, A. Boisen and K.
29 Zór, *ACS Sensors*, 2019, **4**, 398-405.
30
31
32
33
34 121. H. Do, S.-R. Kwon, K. Fu, N. Morales-Soto, J. D. Shrout and P. W. Bohn, *Langmuir*,
35 2019, **35**, 7043-7049.
36
37
38
39
40 122. L. A. Baker, *Journal of the American Chemical Society*, 2018, **140**, 15549-15559.
41
42
43 123. Y.-Y. Peng, R.-C. Qian, M. E. Hafez and Y.-T. Long, *ChemElectroChem*, 2017, **4**, 977-
44 985.
45
46
47
48 124. L. Sepunaru, K. Tschulik, C. Batchelor-McAuley, R. Gavish and R. G. Compton,
49 *Biomaterials Science*, 2015, **3**, 816-820.
50
51
52
53
54
55
56
57
58

- 1
2
3 125. A. Frkonja-Kuczin, L. Ray, Z. Zhao, M. C. Konopka and A. Boika, *Electrochimica Acta*,
4 2018, **280**, 191-196.
5
6
7
8
9 126. L. M. Stabryla, K. A. Johnston, J. E. Millstone and L. M. Gilbertson, *Environmental*
10 *Science: Nano*, 2018, **5**, 2047-2068.
11
12
13
14 127. J. Y. Lee, B.-K. Kim, M. Kang and J. H. Park, *Scientific Reports*, 2016, **6**, 30022.
15
16
17
18 128. E. Lebègue, N. L. Costa, R. O. Louro and F. Barrière, *Journal of The Electrochemical*
19 *Society*, 2020, **167**, 105501.
20
21
22
23 129. A. T. Ronspees and S. N. Thorgaard, *Electrochimica Acta*, 2018, **278**, 412-420.
24
25
26
27 130. G. Gao, D. Wang, R. Brocenschi, J. Zhi and M. V. Mirkin, *Analytical Chemistry*, 2018,
28 **90**, 12123-12130.
29
30
31
32 131. R. A. S. Couto, L. Chen, S. Kuss and R. G. Compton, *Analyst*, 2018, **143**, 4840-4843.
33
34
35
36 132. S. Pirbadian, M. S. Chavez and M. Y. El-Naggar, *Proceedings of the National Academy*
37 *of Sciences*, 2020, **117**, 20171.
38
39
40
41 133. V. Sundaresan, A. R. Cutri, J. Metro, C. S. Madukoma, J. D. Shrouf, A. J. Hoffman, K.
42 A. Willets and P. W. Bohn, *Electrochemical Science Advances*, **n/a**, e2100094.
43
44
45
46
47 134. L. P. Zaino, D. A. Grismer, D. Han, G. M. Crouch and P. W. Bohn, *Faraday Discussions*,
48 2015, **184**, 101-115.
49
50
51
52 135. S. Wang, Y. Zhu, Y. Yang, J. Li and M. R. Hoffmann, *Electrochimica Acta*, 2020, **338**,
53 135864.
54
55
56
57
58

- 1
2
3 136. A. K. Singh, J. Jaiswal and M. Dhayal, *Journal of Electroanalytical Chemistry*, 2020,
4
5 **868**, 114119.
6
7
8
9 137. S. Bergner, J. Wegener and F.-M. Matysik, *Analytical Methods*, 2012, **4**, 623-629.
10
11
12 138. F. Zhao, F. Conzuelo, V. Hartmann, H. Li, S. Stapf, M. M. Nowaczyk, M. Rögner, N.
13
14 Plumeré, W. Lubitz and W. Schuhmann, *Biosensors and Bioelectronics*, 2017, **94**, 433-
15
16 437.
17
18
19
20 139. J. Zhang, T. Zhu, J. Lang, W. Fu and F. Li, *Current Opinion in Electrochemistry*, 2020,
21
22 **22**, 178-185.
23
24
25
26 140. B. Huang, W. Q. Wang, M. Bates and X. W. Zhuang, *Science*, 2008, **319**, 810-813.
27
28
29 141. M. G. L. Gustafsson, *Journal of Microscopy*, 2000, **198**, 82-87.
30

31 **Biographies**

32 **Vignesh Sundaresan**

33
34 Vignesh Sundaresan is an Assistant Research Professor in the Department
35
36 of Chemical and Biomolecular Engineering at the University of Notre
37
38 Dame. He received his bachelor's degree from Central Electrochemical
39
40 Research Institute, India, and Ph.D. in Chemistry from Temple
41
42 University. Prior to his current position, he worked as a postdoctoral
43
44 research associate at the University of Notre Dame. His research focuses on advancing capabilities
45
46 to obtain and understand the behavior of single entities such as molecules, nanoparticles, and
47
48 enzymes to reveal heterogeneity in their properties that are not evident in the ensemble
49
50 measurements.
51
52
53
54
55
56
57
58



Hyein Do

Hyein Do is currently an Analytical Scientist with Entegris in Texas. She received a B.S (Chemistry) from Purdue University and a Ph.D. (Chemistry and Biochemistry) from the University of Notre Dame. Her dissertation concentrates on using Raman spectroscopy with electrochemical techniques to investigate the secretion of virulence factor by *Pseudomonas. aeruginosa* and also to understand the behavior of a common soil bacterium, *Myxococcus xanthus*.

**Joshua D. Shrout**

Joshua Shrout is Professor of Civil & Environmental Engineering and Earth Sciences with an adjunct appointment in Biological Sciences at the University of Notre Dame. His research group investigates single-cell and coordinated behaviors of bacteria such as cell division, heavy metal-binding, EPS production, quorum sensing, flagellar- and type IV-pili mediated motility, and biofilm development. His research is supported by NIH, DOE, and NSF. He currently serves on the Editorial Board for the journals Applied and Environmental Microbiology and Journal of Bacteriology.

**Paul W. Bohn**

Paul W. Bohn is the Arthur J. Schmitt Professor of Chemical and Biomolecular Engineering and Professor of Chemistry and Biochemistry at the University of Notre Dame. He received the B.S. in Chemistry from Notre Dame and the Ph.D. from the University of Wisconsin—Madison. In 1983 he joined the faculty at the University of Illinois at Urbana—



1
2
3 Champaign (UIUC), where he remained until moving to Notre Dame in 2006. His research
4
5 interests include: molecular nanotechnology, integrated micro-nanofluidic chemical
6
7 measurements, and correlated chemical imaging.
8
9
10
11
12
13
14
15
16
17
18
19
20
21
22
23
24
25
26
27
28
29
30
31
32
33
34
35
36
37
38
39
40
41
42
43
44
45
46
47
48
49
50
51
52
53
54
55
56
57
58